Journal of Achievements in Materials and Manufacturing Engineering

VOLUME 19
ISSUE 1
November
2006

Numerical solution techniques for structural instability problems

E. Armentani [a,*], C. Calí [b], G. Cricrí [b], F. Caputo [c], R. Esposito [a]
[a] Department of Industrial Design and Management, University of Naples Federico II, P.le Tecchio 80, 80125 Naples, Italy
[b] Department of Mechanical Engineering, University of Salerno, via Ponte Don Melillo 1, 84084 Fisciano, Italy
[c] Department of Aerospace and Mechanical Engineering, Second University of Naples, Via Roma 29, 81031 Aversa, Italy
* Corresponding author: E-mail address: enrico.armentani@unina.it

Received in revised form 15.07.2006; accepted 30.09.2006

Analysis and modelling

ABSTRACT

Purpose: The purpose is to overcome numerical problems arising in structural instability numerical computations for equilibrium configurations corresponding to increasing loads on structures having points of instability or more generally large non linearity.
Design/methodology/approach: The used numerical methodology was the finite element method with the particular technique of non linear transient dynamic analysis. In such way dynamic equilibrium paths, which are able to lead to required corresponding static ones, can be obtained.
Findings: A methodology to develop this kind of analyses as well as a procedure to set some initial parameters and to check the accuracy of the solution have been investigated and pointed out.
Research limitations/implications: In the future it will be possible to apply the investigated numerical procedure to other practical cases.
Originality/value: We have overcome the limitations in the use of the Newton-Raphson classical method when load control conditions are considered. We also emphasise the practical limits of the Arc Length technique, which requires consistent formulations of the element stiffness matrix in non-linear field; this kind of high precision is often not available in the common FE codes.
Keywords: Arc-length; Buckling; Post-buckling; Quasi-static analysis

1. Introduction

Nowadays, especially in the aeronautical field thinner and thinner panels are used thanks to the availability of very stiff materials by which lighter panels for fuselages can be obtained. This geometrical characterization points out the problem of buckling and structural static equilibrium. Some previous works [1-29], for example, deal with the problem of non-linear static equilibrium taking account of large displacements for thin cylindrical panels in composite material under axial, shear or torsional loads, or material nonlinearity.

The difficulty in determining critical points and reaching equilibrium points on non-stable paths was studied and solved by Wempner and Riks [30-32] in the seventies by using the Arc Length technique, which at present is implemented in various finite element codes commercially available.

The present numerical work deals with the peculiar characteristics of stability and convergence of the Arc Length method and, in particular, with the algorithms available in commercial codes, such as ANSYS and NASTRAN, by which numerical evaluations have been performed. An in-house code [33] has been developed in order to better investigate the method

and its procedural parameters set-up, by means of non-linear analyses of beam structures. These results are successively compared with those obtained by using the aforesaid commercial codes in which these parameters are often not defined by users.
Moreover this study points out the possibility to obtain points of static equilibrium by using the classical FEM algorithms utilized in dynamical solutions [34, 35].

With this assumption we consider the structure, whose degrees of freedom are provided with opportunely chosen damping factors, under loads slowly increasing over a wide interval of time, so that the quasi-static equilibrium path can be confused with the static path determined in the stable intervals. In this way we can reach equilibrium points which otherwise would be difficult to obtain through static analysis.

Finally we show the influence of the parameters set-up on the dynamic solutions and suggest some criteria to determine, with required accuracy, the quasi-static equilibrium path, also reducing the computational effort.

2. Static equilibrium in instability condition

The problem of static equilibrium in geometrically non-linear field within a FEM procedure leads to the following governing equation

$$\boldsymbol{\Phi}(\boldsymbol{u})=\boldsymbol{P} \tag{1}$$

which expresses the balance of the external forces vector $\boldsymbol{P}$ with the nodal forces $\boldsymbol{\Phi}(\boldsymbol{u})$, whose dependence on displacements $\boldsymbol{u}$ is non-linear. The above equilibrium equation is usually solved by Newton-Raphson (NR) or derived methods. This well known technique consists in the solution of a series of linear equations as follows

$$\boldsymbol{K}(\boldsymbol{u}^i)\boldsymbol{\Delta u}^{i+1}=\boldsymbol{P}-\boldsymbol{\Phi}(\boldsymbol{u}^i), \tag{2}$$

where $\boldsymbol{u}^i$ represents the i-th approximation of the solution $\boldsymbol{u}$; $\boldsymbol{K}(\boldsymbol{u}^i)$ is the matrix containing the derivatives of the internal forces vector $\boldsymbol{\Phi}(\boldsymbol{u})$ with reference to each term of the vector $\boldsymbol{u}$, evaluated in the point $\boldsymbol{u}^i$; finally, $\boldsymbol{P}-\boldsymbol{\Phi}(\boldsymbol{u}^i)$, are the so called residual forces which determine the increment $\boldsymbol{\Delta u}^{i+1}$ of displacements. At every iteration the vector $\boldsymbol{u}^i$ is updated as $\boldsymbol{u}^{i+1} = \boldsymbol{u}^i + \boldsymbol{\Delta u}^{i+1}$ and the other derived quantities are consequentially changed. We consider that the convergence is recovered when the residual forces become smaller than an assigned value; if the matrix $\boldsymbol{K}$ of derivatives, which coincides with the tangent stiffness of the structure, holds his positive definitiveness, the procedure is convergent and the convergence is quadratic.

The Arc Length (AL) method, originally introduced by Wempner [30] and Riks [31, 32], and treated, among others, by Crisfield [36-40] is apt to follow equilibrium paths which offer unstable points, where it is not possible to find solutions of eq. (1) with NR techniques. The AL method consists in the solution of the non-linear incremental system given by the following equations

$$\boldsymbol{G} = \boldsymbol{\Phi}(\boldsymbol{u} + \boldsymbol{\Delta u}) - (\lambda + \Delta\lambda)\boldsymbol{P}^* = \boldsymbol{0} \tag{3a}$$

$$g = \boldsymbol{\Delta u}^T\boldsymbol{\Delta u} + \psi^2\Delta\lambda^2 = \rho^2 , \tag{3b}$$

where the vector ($\boldsymbol{u}$; λ) represents the currently calculated equilibrium point, λ is the reference load $\boldsymbol{P}^*$ multiplier and ψ an opportunely chosen scale factor. The last equation requires that the vector ($\boldsymbol{\Delta u}$; $\psi\Delta\lambda$) norm gets a fixed value ρ; this means that the point ($\boldsymbol{u} + \boldsymbol{\Delta u}$; $\lambda + \Delta\lambda$) belongs to a quadratic hypersurface $\mathscr{H}$ centered in ($\boldsymbol{u}$; λ). The system of eq. (3), provided that the hypersurface parameter ρ is small enough, is stable and it is possible to obtain the solution by means of NR algorithms also for paths describing physically unstable equilibrium. It is appropriate and sometimes necessary to employ this technique; for example, in presence of a limit point in which the stiffness matrix is singular, it would be necessary to gradually reduce the load step by using the conventional NR technique. In this case the load increment is given by the quantity $\Delta\lambda\boldsymbol{P}^*$, which decreases automatically when the limit point is approximated; this is due to the constraint imposed by the eq. (3b) at the same time without influencing neither the stability of the algorithm nor the fastness of convergence. When it is necessary to overcome an unstable zone to verify the presence of further stable branches along the whole equilibrium path, the use of AL could be necessary if the distance between two stable branches would make impossible or too difficult the convergence of the eq. (1). Anyway the use of this technique becomes absolutely necessary if, for any reason, it is relevant to know the behaviour of an unstable piece of equilibrium path.

3. Resolutive techniques for the Arc-Length method

The Newton-Raphson method applied to the system of eq. (3) leads to the following equations

$$\begin{bmatrix} \boldsymbol{K}(\boldsymbol{u}+\Delta\boldsymbol{u}^i) & -\boldsymbol{P}^* \\ 2(\Delta\boldsymbol{u}^i)^T & 2\psi^2\Delta\lambda^i \end{bmatrix}\begin{bmatrix} \delta\boldsymbol{u}^{i+1} \\ \delta\lambda^{i+1} \end{bmatrix} =$$

$$= \begin{bmatrix} -\boldsymbol{\Phi}(\boldsymbol{u}+\Delta\boldsymbol{u}^i)+(\lambda+\Delta\lambda^i)\boldsymbol{P}^* \\ \rho^2-(\Delta\boldsymbol{u}^i)^T(\Delta\boldsymbol{u}^i)-\psi^2(\Delta\lambda^i)^2 \end{bmatrix} = \begin{bmatrix} -\boldsymbol{G}^i \\ \rho^2-g^i \end{bmatrix} \tag{4}$$

The results are the increments $\delta\boldsymbol{u}^{i+1}$ e $\delta\lambda^{i+1}$ corresponding to the i-th approximation of the solution. Even if the stiffness matrix of the structure is singular, the matrix of derivatives is, generally, non-singular; this property allows the iterative algorithm to hold its convergence capabilities also on unstable segments of the equilibrium path. But, unlike the matrix $\boldsymbol{K}$, it is neither symmetric nor banded; in order to avoid this inconvenient, which does not allow the usage of standard solution processors usually employed for structural analysis with FEM, we can resort, for example, to the technique suggested by Crisfield. From the eq. (4) the displacements increment is obtained in the form

$$\delta\boldsymbol{u}^{i+1} = -\boldsymbol{K}^{-1}(\boldsymbol{u} + \boldsymbol{\Delta u}^i)\boldsymbol{G}^i + \delta\lambda^{i+1}(\boldsymbol{K}^{-1}(\boldsymbol{u} + \boldsymbol{\Delta u}^i)\boldsymbol{P}^*) =$$

$$= \delta\boldsymbol{u}^I + \delta\lambda^{i+1}\delta\boldsymbol{u}^{II} . \tag{5}$$

By using the second of eq. (3) written for the two successive iterations i and i+1, and imposing that successive approximations of the solution lie on the hypersurface $\mathcal{K}$ we obtain the expression

$$(\boldsymbol{\Delta u}^{i+1})^{\mathbf{T}}\boldsymbol{\Delta u}^{i+1} + \psi^2(\Delta\lambda^{i+1})^2 =$$

$$= (\boldsymbol{\Delta u}^{i})^{\mathbf{T}}\boldsymbol{\Delta u}^{i} + \psi^2(\Delta\lambda^{i})^2 = \rho^2 \tag{6}$$

then, after the substitution of $\boldsymbol{\Delta u}^{i+1}$ e $\Delta\lambda^{i+1}$ respectively given by the relations

$$\boldsymbol{\Delta u}^{i+1} = \boldsymbol{\Delta u}^{i} + \delta\boldsymbol{u}^{I} + \delta\lambda^{i+1}\delta\boldsymbol{u}^{II}$$

$$\Delta\lambda^{i+1} = \Delta\lambda^{i} + \delta\lambda^{i+1} \tag{7}$$

we get the following quadratic expression in the variable $\delta\lambda^{i+1}$, which makes it possible to evaluate definitively the increment of the displacement vector

$$a(\delta\lambda^{i+1})^2 + b\delta\lambda^{i+1} + c = 0 \tag{8}$$

where

$$a = (\delta\boldsymbol{u}^{II})^T\delta\boldsymbol{u}^{II} + \psi^2$$

$$b = 2((\boldsymbol{\Delta u}^{i} + \delta\boldsymbol{u}^{I})^T\delta\boldsymbol{u}^{II} + \psi^2\,\Delta\lambda^{i})$$

$$c = (\boldsymbol{\Delta u}^{i} + \delta\boldsymbol{u}^{I})^T(\boldsymbol{\Delta u}^{i} + \delta\boldsymbol{u}^{I}) + \psi^2\,\Delta\lambda^{i} - \rho^2.$$

By using this technique the operations of factorization on the augmented matrix do not have to be performed and then the computational effort for the single iteration is not so different from the one which is necessary to solve only the eq. (1).
An approximate solution technique [41] consists in evaluating $\delta\lambda^{i+1}$ by using the following linear expression

$$\delta\lambda^{i+1} = \frac{\alpha^i - (\Delta\boldsymbol{u}^i)^T\,\delta\boldsymbol{u}^I}{\psi^2\Delta\lambda^i + (\Delta\boldsymbol{u}^i)^T\,\delta\boldsymbol{u}^{II}} \tag{9}$$

where the scalar quantity α^i may be defined in some different ways. The simplest criterion is to impose $\alpha^i = 0$. In this way the increment $\delta\lambda^{i+1}$ is defined by the equivalent expression

$$(\boldsymbol{\Delta u}^{i};\,\psi\Delta\lambda^{i}) \times (\delta\boldsymbol{u}^{i+1};\,\psi\delta\lambda^{i+1}) = 0,$$

that is an orthogonal relationship between the (i+1)-th increment vector and the i-th approximation of the incremental solution vector. Such an easier solution does not oblige us to choose at every iteration, between the two solutions of eq. (8), the one leading towards the right direction of the equilibrium curve.

On the contrary, it is less stable than the previous one, obliging sometimes to reduce considerably the value of the parameter ρ. Actually the evaluation of the increment of the load parameter according to the eq. (9), without considering exactly the eq. (3b), does not constrain the i-th approximation of the equilibrium point to lie on the aforesaid hypersurface; in this way it is possible, with the subsequent iterations, that the norm of the vector ($\boldsymbol{\Delta u}$; $\psi\Delta\lambda$) becomes also very different from the initial value ρ, causing the partial loss of stability benefit obtainable by the Arc Length technique.
By writing the constraint (3b) in the following equivalent way

$$g' = (\boldsymbol{\Delta u}^T\boldsymbol{\Delta u} + \psi^2\Delta\lambda^2)^{(1/2)} = \rho,$$

the corresponding incremental equation is written

$$\begin{bmatrix} \boldsymbol{K}(\boldsymbol{u}+\Delta\boldsymbol{u}^i) & -\boldsymbol{P}^* \\ \Delta\boldsymbol{u}^i / g'^i & \psi^2\Delta\lambda^i / g'^i \end{bmatrix}\begin{bmatrix} \delta\boldsymbol{u}^{i+1} \\ \delta\lambda^{i+1} \end{bmatrix} =$$

$$= \begin{bmatrix} -\boldsymbol{\Phi}(\boldsymbol{u}+\Delta\boldsymbol{u}^i) + (\lambda+\Delta\lambda^i)\boldsymbol{P}^* \\ \rho - (\Delta\boldsymbol{u}^i)^T(\Delta\boldsymbol{u}^i) - \psi^2(\Delta\lambda^i)^2 \end{bmatrix} = \begin{bmatrix} -\boldsymbol{G}^i \\ \rho - g'^i \end{bmatrix}$$

by which we finally obtain the increment

$$\delta\lambda^{i+1} = \frac{(\rho - g'^i)g'^i - (\Delta\boldsymbol{u}^i)^T\,\delta\boldsymbol{u}^I}{\psi^2\Delta\lambda^i + (\Delta\boldsymbol{u}^i)^T\,\delta\boldsymbol{u}^{II}} \tag{10}$$

that has the same form of eq. (9).

This technique leads to an equilibrium solution close to the one derived from the Crisfield algorithm with the advantage of using a linear expression for the increment.

For the following application examples it has been applied, among the others, an "in-house" solver based on the described technique.

4. Numerical investigation on the Arc Length method

Some analyses of simple structures have been made whose equilibrium paths show unstable zones, by using in these cases the finite elements code ANSYS 5.7 and the aforesaid in house code. The structure of Fig. 1, whose SPAR elements present axial stiffness only, is provided with only two degrees of freedom and its equilibrium path can be calculated also analytically according

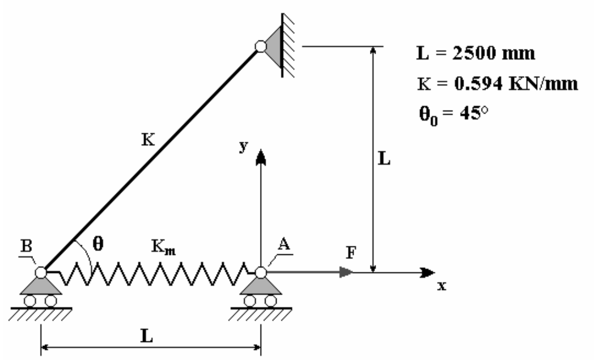

Fig. 1. Simple snap-back or snap-through schema. to the following parametric expression referred to the x direction

$$F_B = -K(l_1(u_B)-l_1(0))\cos(\theta(u_B)) = F_A = F$$

$$u_A = u_B + F/K_m \qquad (11)$$

where $l_1(u_B) = (L^2 + (u_B - L)^2)^{(1/2)}$ is the current length of the initially inclined bar, $\cos(\theta(u_B)) = (L - u_B)/l_1(u_B)$ the projection of the same bar on the x axis, F_A and F_B the nodal forces in direction x and u_A and u_B the corresponding displacements.

The cylindrical shell whose characteristics are shown in Fig. 2, has been discretised by using quadratic shell elements available in the ANSYS library limiting, for simplicity sake, the analysis to a quarter of the structure. The straight sides have all the d.o.f. 's constrained except the rotations around the direction parallel to the cylinder axis. This kind of behaviour of the examined structure has been numerically evaluated, for different values of the shell thickness, by Crisfield [36] and Surana [42].

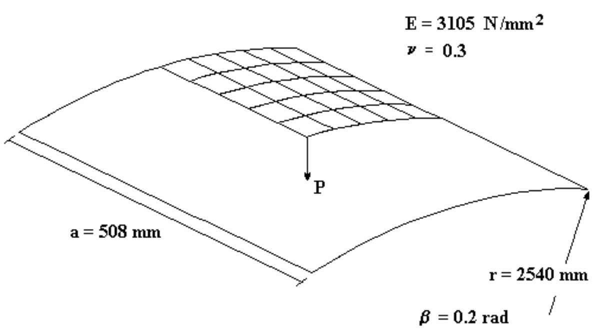

Fig. 2. Cylindrical shell with unstable behaviour [36]

Finally, the structure shown in Fig. 3, is made up of beam elements with square section and is constrained and loaded just like the previous one.

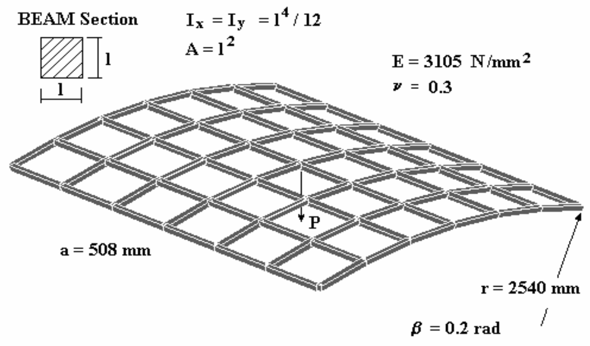

Fig. 3. Beam-made shell with unstable behaviour [33]

The equilibrium paths of the first analyzed structure (Figs. 4 and 5) always show a snap-through, when the ratio K_m/K between the rod stiffness changes, and a contemporary snap-back might be present. The latter possibility occurs when K_m/K becomes lower than $\sqrt{2}$-1, as the analytical expression (11) of the same path shows.

The analysis by finite elements with the Arc-Length technique implemented in the ANSYS code reveals more and more convergence difficulties when this ratio gets smaller. It has been found that, for the analyzed structure ρ_{max} is a crucial parameter for the convergence. For $K_m/K = 1$ (Fig. 4) the snap-back does not take place and the convergence is reached by assuming ρ_{max} less than the one corresponding to an initial increment of the load multiplier λ equal to about 1/20; on the contrary if the ratio $K_m/K = 0.28$ (Fig. 5) it is necessary, in order to recover the whole equilibrium path without inversion of direction, to set up the initial increment of λ equal at most to 1/2000, because the algorithm becomes unstable for bigger load steps.

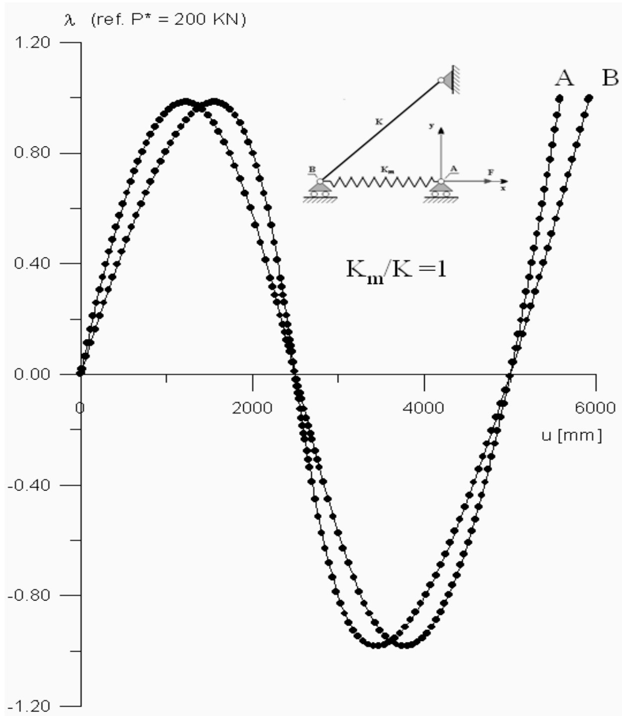

Fig. 4. Equilibrium path of the first schema without snap-back

The cylindrical shell structure presents a behaviour strongly influenced by the thickness. When the thickness is t=12.7 mm (Fig. 6) the case may be solved by setting up the displacement increment of the central node A and then verifying the reaction; but if we want to impose directly the force, it is necessary to use the Arc Length method owing to the presence of snap-through. In this second case we can identify, without any relevant difficulty, the equilibrium path with a large possibility to choose the initial parameters. If the shell thickness is t=6.35 mm (Fig. 7) the use of Arc-length method is compulsory owing to the presence of the snap-back. In this case the choice of the calculation options, and in particular of the initial value of ρ, ρ_0, and the maximum allowed value ρ_{max}, greatly influences the convergence of the solution, even if it has been reached without too many difficulties. The results shown in the Figures are in good agreement with those presented in [36] and [39].

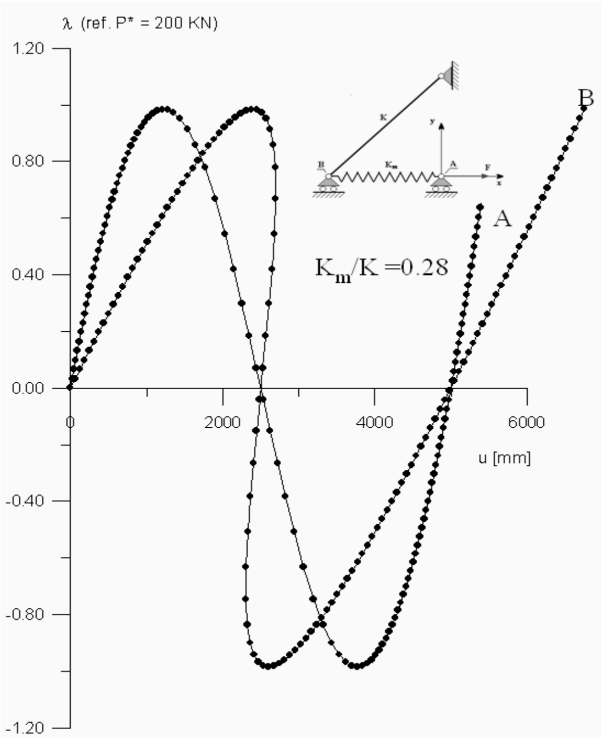

Fig. 5. Equilibrium path of the first schema with snap-back

The equilibrium paths of the third kind of structure (Figs. 8 - 11) show a qualitative behaviour very similar to that of the shell. Also in this case, when the geometrical parameter l diminishes, we proceed from easily identified paths with only snap through to paths with characteristics of more difficult numerical convergence which in addition present snap-back or quite "curling".

For $l = 16$ mm the analysis does not present any difficulty and the convergence may be reached by large field of initial parameters variation. If we put $l = 9$ mm we can point out the presence of a marked snap-back. In this case the difficulties of the analysis convergence are certainly higher by using the ANSYS code: only by setting up a load step number included between 90 and 110 we can redraw the entire equilibrium curve. If the step number is higher than 110 the return to the already evaluated path occurs; but if the mentioned number is less than 90 the instability of the iterative procedure appears with an untimely jump on the second stable branch as soon as the trend towards the snap-back effect starts to be considerable. Besides, also in the case in which the critical zone is overcome, the equilibrium points are not evaluated in succession along the curve, but they are the results of numerous changes of direction which stop only after many load steps, allowing in this way to go on following the path.

By reducing the value of l (Figs.10 and 11), in spite of numerous tests performed varying each initial parameter, the ANSYS solver has not been able to overcome the first snap-back. In some cases, by adequately increasing the number of load steps, we can anyway obtain the convergence; but as this problem involves a number of dof's equal about to fifty and the number of necessary steps is estimated to be of magnitude order of hundreds of thousands it is difficult to get results in reasonable time.

The plots related to this kind of structure also show equilibrium paths evaluated by the in-house solver. The elaborated solver, also endowed with the ability of the load step agreement to the curvature of the equilibrium path, presents the best stability qualities being able to point out, without any difficulty and with a reduced number of load steps complicated paths just like those shown in Figs. 10 and 11.

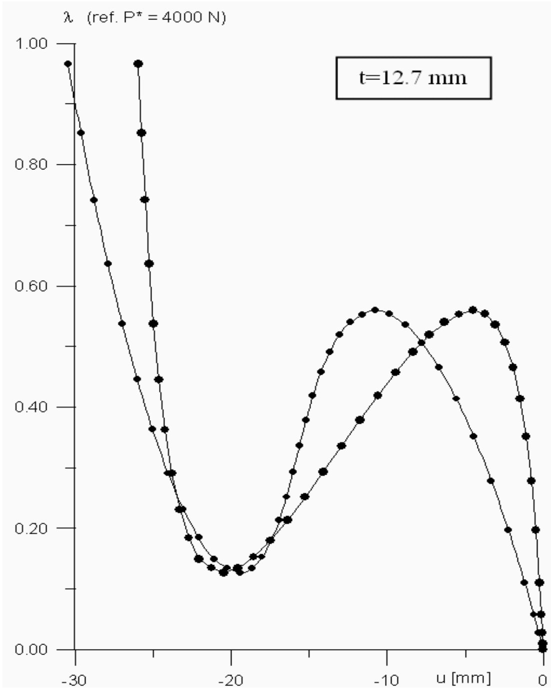

Fig. 6. Equilibrium path of a thick cylindrical shell

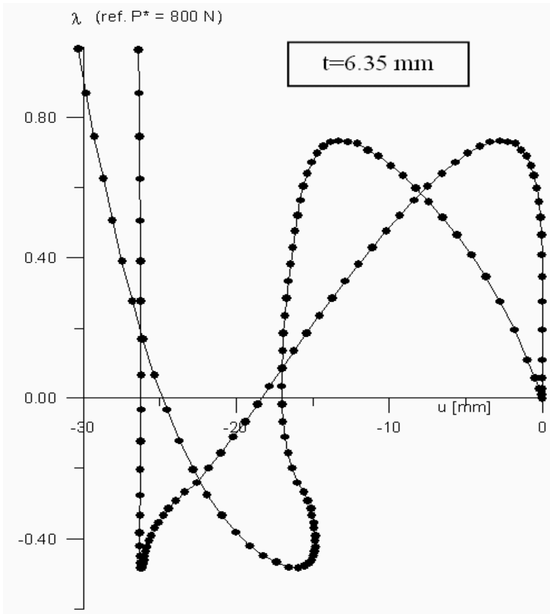

Fig. 7. Equilibrium path of a thin cylindrical shell

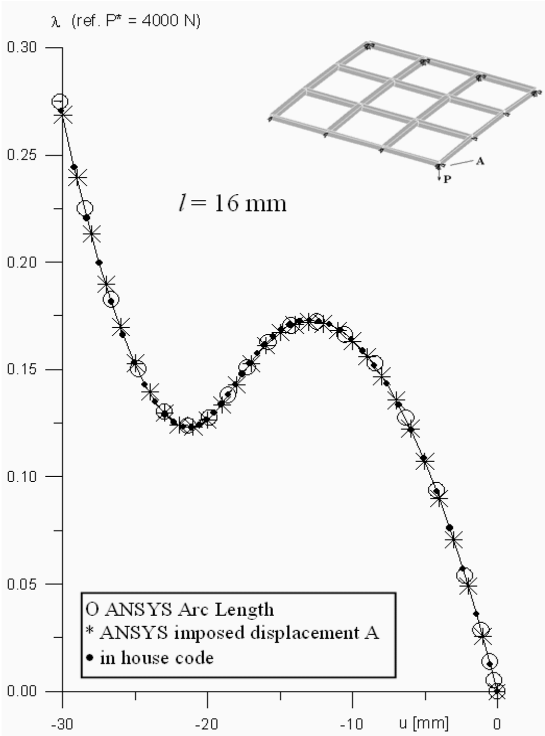

Fig. 8. Thick structure: only snap-through is present

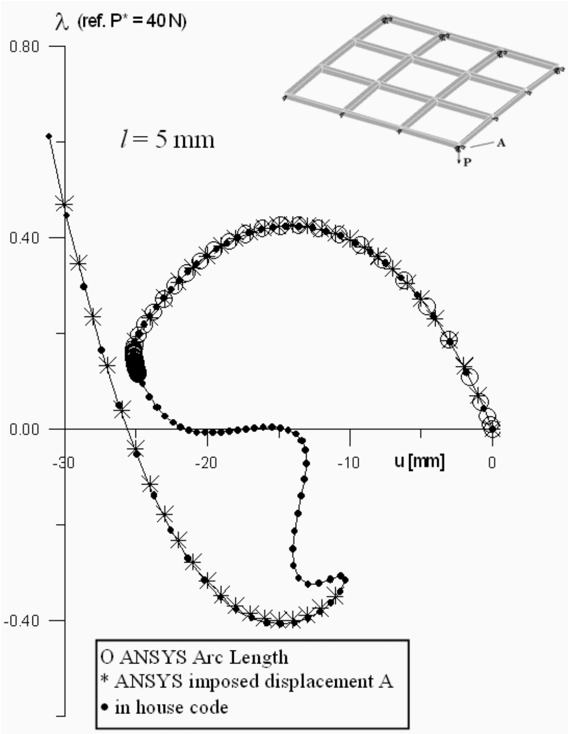

Fig. 10. Thin structure equilibrium path

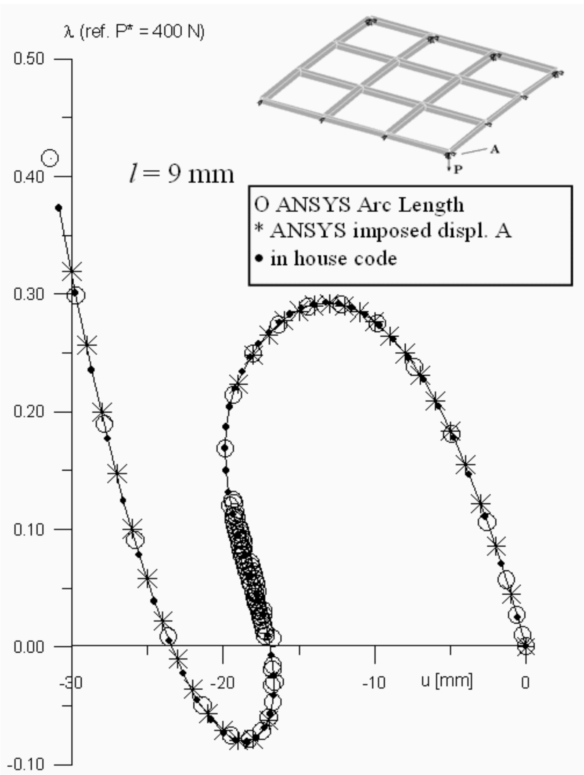

Fig. 9. Moderately thick structure: snap-back is present

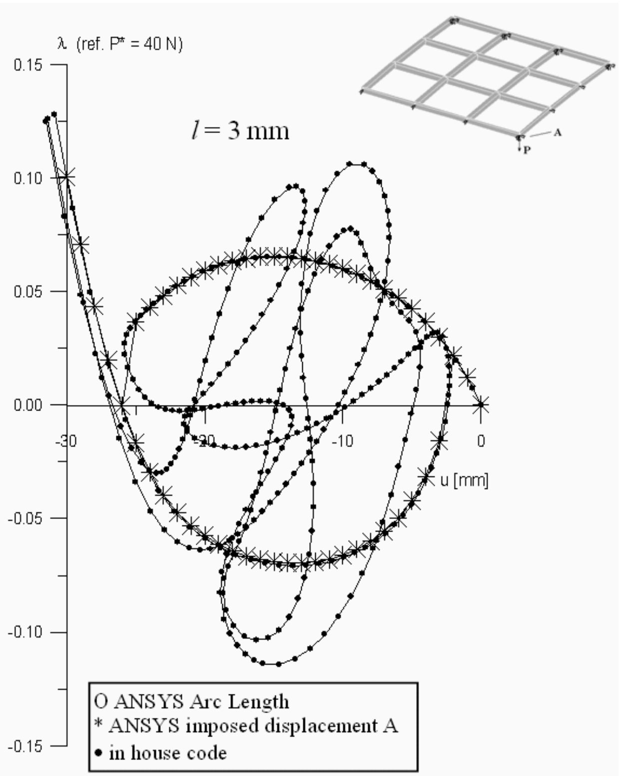

Fig. 11. Very thin structure equilibrium path

5. Analysis of results

The option of non-linear static evaluation of results by the Arc Length method, implemented in commercial FE codes, generally implies the possibility of using a certain number of parameters among those we discussed in the previous paragraphs. Four or five instructions are usually included which allow the definition of these parameters: three of them define the initial length ρ_0, the maximum ρ_{max} and the minimum ρ_{min} of the parameter ρ, while the others are indirectly present through their influence on the automatic optimization procedure of this length. The careful choice of these parameters determines not only the number of equilibrium points which are evaluated and the computation times, but also the same length of the curve, in the domain ($\boldsymbol{u}$; λ) revealed before convergence difficulties arise.

For example, if the particular shape of the path needs, for the automatic adaptive procedure, smaller and smaller load steps, the analysis will be stopped when the lowest fixed length of the arc radius has been reached. In this case, if it is possible, we must restart the analysis starting from the latest found equilibrium point, after varying opportunely the initial parameters.
On this subject, in order to utilize efficiently the restart option, it is suitable that the restart point of the new analysis lies on a stable zone of the equilibrium curve. On the contrary we introduce a strong instability reason in the iterative algorithm which cannot be always overcome.

Moreover, convergence problems may arise which can be avoided with much more difficulties because of instability caused by the use of the relation (9) instead of (8) in evaluating the increment of the load parameter. In some cases this increment offers an uncontrolled increasing modulus while the iterations in the same load step proceed as far as to reach the maximum allowed values by the initial parameters. At this point the automatic bisection procedure of the radius ρ is carried out; but it is not able in every case to solve this instability condition and performs successive bisections as far as the value ρ_{min} is reached and the analysis stops without reaching the convergence.

We can attempt to solve the problem by varying the initial amplitude of the load step and/or ρ limits, which could turn out to be too large or too small. Anyway we must point out that the same instability may lead to the individuation of an equilibrium point also very far from the starting point in spite of the constraint imposed to the load and displacement increments, especially if an excessive value for the parameter ρ_{max} is chosen.

A typical erroneous trend of the method, present *in nuce* already in the quadratic formulation lying on the hypersurface $\mathscr{H}$ (eq. 3b), consists in the tendency to evaluate equilibrium points belonging to the already evaluated path. Usually the commercial codes offer a check routine capable to point out in many cases this difficulty and to attempt a solution by dividing the currently imposed value of ρ.

But sometimes the mistake is not pointed out and the analysis proceeds without interruptions running over the already determined whole path. In these cases the analysis must be repeated from the starting point after varying the solution parameters or stopping the computation before the inversion in order to try, if it is possible, a further restart.

6. Procedure parameters for dynamical transient analysis

From the discussion presented in the previous sections, it is possible to infer that the convergence problems arising around the critical points durig the static analysis are caused essentially by ill-conditioning of the stiffness matrix $\boldsymbol{K}$. If there is not the possibility to use an alternative solver, this situation can be avoided by using solution algorithms of dynamic transients in the way that we will expose in what follows.

It is worth noting that the dynamical transient analysis implies the determination of the dynamical response of a structure to any time-dependent load for which any step by step configuration of the examined structure will be influenced not only by the same load but also by the mass and damping distribution.
Referring to finite element formulation, the governing equation of dynamical equilibrium in matrix form is written as

$$\mathbf{M}\ddot{u} + \mathbf{C}\dot{u} + \mathbf{\Phi}(u) = \mathbf{F}(\mathrm{t}), \qquad (12)$$

where

$\mathbf{M}$ is the mass matrix,
$\mathbf{C}$ is the damping matrix,
$\mathbf{\Phi}$ is the nodal force vector,
$\ddot{u}$ is the nodal accelerations vector,
$\dot{u}$ is the nodal velocities vector,
u is the nodal displacements vector,
$\mathbf{F}(\mathrm{t})$ is the nodal loads vector.

In order to utilize the algorithms of dynamic transients to obtain static equilibrium points which contain unstable zones, it is necessary that the forces deriving from the presence of masses and dissipations are reduced up to the quasi static equilibrium by searching, at the same time, the maximum efficiency in the computational effort in terms of times and then in terms of total number of iterations.

Quantities parameters for solving algorithm on which we can operate to achieve the above mentioned results are:

a) the damping matrix $\mathbf{C}$, depending on the damping value imposed to the system as internal damping of the material or, similarly to the examined case, as α and β defined in what follows;
b) the mass matrix $\mathbf{M}$, easily to control by means of value of material density, or eventually, of lumped masses;
c) the time interval of the load application and the imposed integration step Δt.

7. Determination of procedure parameters

In order to develop the dynamical analysis whose aims are discussed in the previous paragraphs, the parameters in the procedure listed above must be opportunely determined taking in account some considerations.

First, in order to obtain a good approximation to static solution it is necessary to introduce some damping to contrast the effect of inertial forces. But relatively high damping could cause the increasing of computational times because it would take a longer time to reduce the effect of velocity dependent forces. The ideal goal would be to introduce a damping which is a little higher than the critical damping of the system in the frequency band mostly excited during the loading process.
The damping matrix, as it is well known, usually may be defined as

$$\mathbf{C} = \alpha\,\mathbf{M} + \beta\mathbf{K}$$

where the values of α and β must be externally imposed and influence each vibration mode by determining the relative damping coefficient ξ_i, equal to ratio between the effective and the critical damping.

If ω_i is the natural angular frequency of the i-th mode, α and β satisfy the relation

$$\xi_i = \alpha/2\omega_i + \beta\,\omega_i/2. \tag{13}$$

To the aim of the developed investigation, we assume, as usual, that the damping factor ξ is approximately constant and slightly higher than the unity (e.g. 1.01) in a defined frequency band; so, given ξ and an interval of frequencies $\omega_i \div \omega_j$, we obtain a system of two equations with two unknowns α e β which are

$$\alpha = 2\,\xi\,\omega_i\,\omega_j\,/\,(\omega_i + \omega_j)$$

$$\beta = 2\,\xi\,/\,(\omega_i + \omega_j). \tag{14}$$

With regard to the forces depending on mass distribution, by changing the matrix [M] operating on the material density or multiplying by a constant term the value of lumped masses, we only modify the time scale without influencing the final result.

Finally, some considerations must be pointed out concerning the algorithm of Newmark [43] utilized in the dynamical calculations; the procedure is based on the well known recursive relation

$$\{\dot{u}_{n+1}\} = \{\dot{u}_n\} + [(1-\delta)\{\ddot{u}_n\} + \delta\{\ddot{u}_{n+1}\}]\Delta t$$

$$\{u_{n+1}\} = \{u_n\} + \{\dot{u}_n\}\Delta t + \left[\left(\frac{1}{2} - \varsigma\right)\{\ddot{u}_n\} + \alpha\{\ddot{u}_{n+1}\}\right]\Delta t^2$$

where

ζ, δ are the Newmark integration parameters,
$\Delta t = t_{n+1} - t_n$,
$\{u_n\}$ is the nodal displacement vector at time t_n,
$\{\dot{u}_n\}$ is the nodal velocity vector at time t_n,
$\{\ddot{u}_n\}$ is the nodal acceleration vector at time t_n,
$\{u_{n+1}\}$ is the nodal displacement vector at time t_{n+1},
$\{\dot{u}_{n+1}\}$ is the nodal velocity vector at time t_{n+1},
$\{\ddot{u}_{n+1}\}$ is the nodal acceleration vector at time t_{n+1}.
From these relations we obtain the governing equation in the unknown $\{u_{n+1}\}$

$$(a_0[M] + a_1[C] + [K])\{u_{n+1}\} = \tag{15}$$

$$= \{F^a\} + [M](a_0\{u_n\} + a_2\{\dot{u}_n\} + a_3\{\ddot{u}_n\}) + [C](a_1\{u_n\} + a_4\{\dot{u}_n\} + a_5\{\ddot{u}_n\})$$

where

$$a_0 = \frac{1}{\varsigma\Delta t^2} \qquad a_1 = \frac{\delta}{\varsigma\Delta t} \qquad a_2 = \frac{1}{\varsigma\Delta t}\ a_3$$

$$a_3 = \frac{1}{2\varsigma} - 1 \qquad a_4 = \frac{\delta}{\varsigma} - 1 \qquad a_5 = \frac{\Delta t}{2}\left(\frac{\delta}{\varsigma} - 2\right)$$

The overcoming convergence problems, as already emphasized, around the critical points during the static analysis are caused by the ill-conditioning of the stiffness matrix **K**. We can avoid this difficulty during the dynamical transient analysis by choosing an opportunely small time integration step Δt. In fact, by replacing the mentioned constant values in the multiplying matrix of the displacement vector, in which we assumed $\zeta = 1/4$ and $\delta = 1/2$ [44], we obtain the matrix

$$\left(\frac{1}{4\Delta t^2} + \frac{2\alpha}{\Delta t}\right)[M] + \left(1 + \frac{2\beta}{\Delta t}\right)[K] = [K^*]\,,$$

whose first term, with positive determinant, increases when Δt diminishes and/or when α also increases.

The influence of Newmark parameters on good conditioning of stiffness matrix $\mathbf{K}^*$ is inferred from the same eq. (15); this conditioning is improved when ζ decreases and when δ increases. It is worth noting that the algorithm is unconditionally stable if the limitations described in [44] are satisfied.

If we want to obtain a quasi-static solution by means of the eq. (12), the dynamic terms, dependent on velocity and acceleration, must be negligible with regard to the static term $\mathbf{\Phi}(u)$. This condition should be formulated, by introducing a norm rate, as follows

$$\Theta = \|\,\mathbf{M}\ddot{u} + \mathbf{C}\dot{u}\,\| \,/\, \|\,\mathbf{\Phi}(u)\,\| < \varepsilon. \tag{16}$$

The calculation of the check parameter Θ, by which it is possible to establish the accuracy of the quasi-static solution, is performed, within this work, by using an opportunely developed Fortran routine.

8. Numerical investigations on quasi-static analysis

By describing the following applications we can define the different steps necessary for the development of the investigation by pointing out every time the influence and the causes of the choice of different parameters examined in the previous section and comparing the results with known numerical solutions. The first case we examined is the thin shell already shown in Fig. 2.

Some considerations concerning a right setting of different parameters which influence the dynamical transient analysis we discussed about in the previous sections must be added.

In order to determine α and β parameters, it is convenient to develop first of all a preliminary harmonic analysis from which derive the frequency response of amplitudes of different displacements of the structure under sinusoidal load of amplitude equal to the maximum value of the applied load with an opportunely small damping (Fig. 12). By this analysis it will be possible to determine what are the natural frequencies of the system mainly excited by the application of the imposed type of load.

Thus it will be possible to identify the frequency band in which we can assume a constant value of the damping factor ξ, in such a way as to damp all the unwanted structural vibrations.

In problems in which the non-linearity highly affects the natural frequency value and in particular in cases which involve static instability of the structure, as in the treated case, it has to be remarked that sometimes natural frequencies of the system, different from the ones evaluated by harmonic analysis, will be detected.

If we choose a frequency band ranging between the first and the n-th significant natural frequencies, those less than the first one which have effect around the critical point will be strongly damped. In these cases, also considering the arbitrariness in assuming the maximum significant frequency, we refer only to the first resonance frequency, by posing in (14) $\omega_i = \omega_j = \omega_1$.

The value of the first natural frequency of the system gives, for the examined case, the damping coefficients α = 12.2 sec^{-1} e β = 0.084 sec.

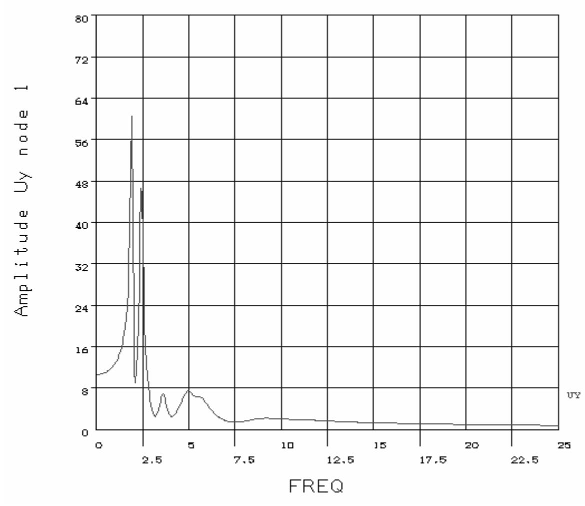

Fig. 12. Frequency response of the cylindrical shell

By using these damping coefficients and assuming a time interval for the application of the load equal to about 40 times the period of the first vibration mode of the structure ($T_1 \approx$ 0.5sec), by dynamic analysis equilibrium points are obtained and shown in Fig. 13.

In the same Figure it is possible to compare these points with the static equilibrium curve, previously obtained by using the Arc Length method.

The second analysed case is a typical stiffened thin panel, whose geometrical and structural characteristics have been reported in Fig. 14. The static solutions shown, among the dynamic ones, in Fig. 15, have been obtained by using the Arc Length method, by means of the MSC NASTRAN code. It presents a principal equilibrium path and two secondary ones determined by using different initial parameters set-up.

While analysing the results obtained by the developed investigation, shown in Figs. 13 and 15 it is necessary above all to point out that, by considering the dynamical approach of the problem, it is not possible to determine the unstable equilibrium points related to the snap-back part of the curve; on the other hand these points may not have any particular significant engineering meaning. So by drawing the equilibrium curve obtained by the dynamical approach we observe that the snap-back phase of the structure is completely overcome, directly jumping from the pre-buckling to the post-buckling phase.

In the first examined case, in which there is the possibility to make comparisons with the static equilibrium path a very good agreement between the two solutions, static and dynamic, is shown. In the second case the static analysis has revealed three different equilibrium paths, and there is no guarantee that others are not present. Two dynamic analyses were performed, the first one with high damping coefficients in order to get a quasi-static solution, the other one with a small damping that returns a full dynamic solution. The quasi - static solution is close to a part of the three branches of the revealed static path, jumping without loss of continuity from a static path to the following one. The full dynamic solution presents a quite similar path, quantitatively, to the quasi-static and the changes of configuration corresponding to the different static branches occur at about the same values of the external force.

In order to ensure the accuracy of the solution, as above mentioned, we must perform the analysis of the components of nodal forces due to mass and damping contributes by verifying that they are relatively small compared with the total value of the correspondent nodal force.

By evaluating the check parameter Θ, the norm of non-static components of the nodal force is shown in graphical form versus the load application time in Fig. 16.

It is possible to infer that it is less than 1% of the applied load value during a large part of the loading process; it is of about the same value in the initial part of the curve, where remarkable non-linearity phenomena do not take place and so it would be easily valuable by static approach by simply eliminating the dynamical effects of the transient resolutive algorithm. In the part corresponding to the snap-back, where, as above said, it is not possible to obtain significant equilibrium points, the defined norm offers relatively high values.

Obviously the greater is the loading time interval, the less are the damping effects and the greater the computing times; for this reason the choice of the time parameter must be made by averaging between the accuracy and the corresponding computing time. Proceeding in this way offers the considerable advantage that each convergence point represents an equilibrium point near to the static one with an approximation valuable in the discussed way.

With reference to the second case, the quasi-static solution (obtained by means of the ANSYS code) is in good agreement with the static solution too, and the transition from an equilibrium path to another appears to be continuous. The dynamic solutions, developed with a very small damping factor, seem to verify the fact that the transition between the different equilibrium paths is well suited.

The use of this technique can be necessary in order to overcome unrecoverable convergence problems of the static analysis. Moreover when more equilibrium paths are obtainable, it permits the continuous transition among them; this seems to develop similarly to the real phenomena.

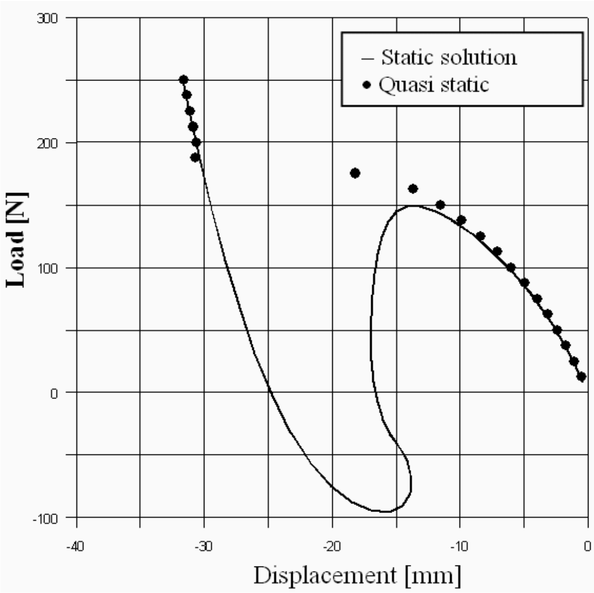

Fig. 13. Static vs quasi static equilibrium path (cyl. shell)

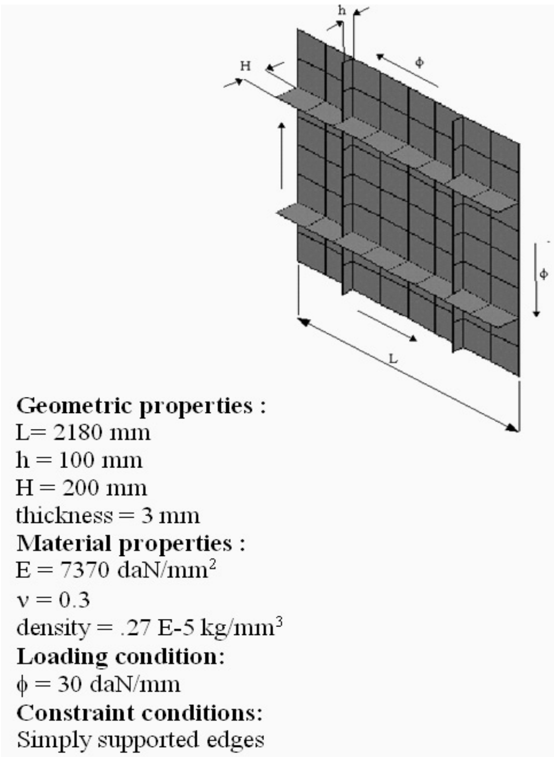

Fig. 14. FE model of a stiffened panel

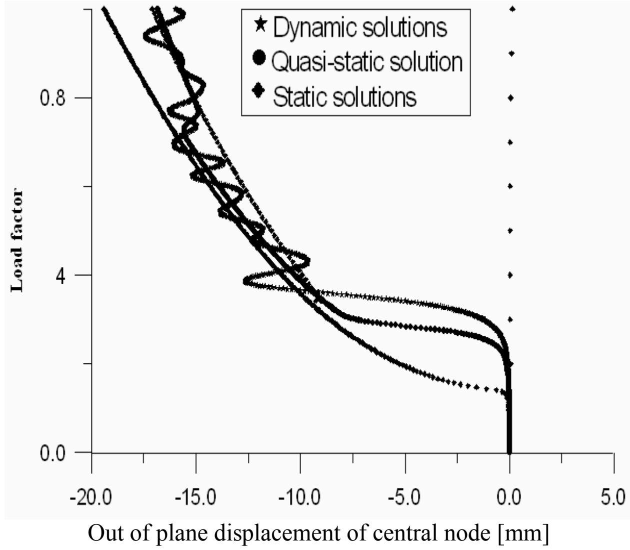

Fig. 15. Comparisons of stiffened panel equilibrium paths

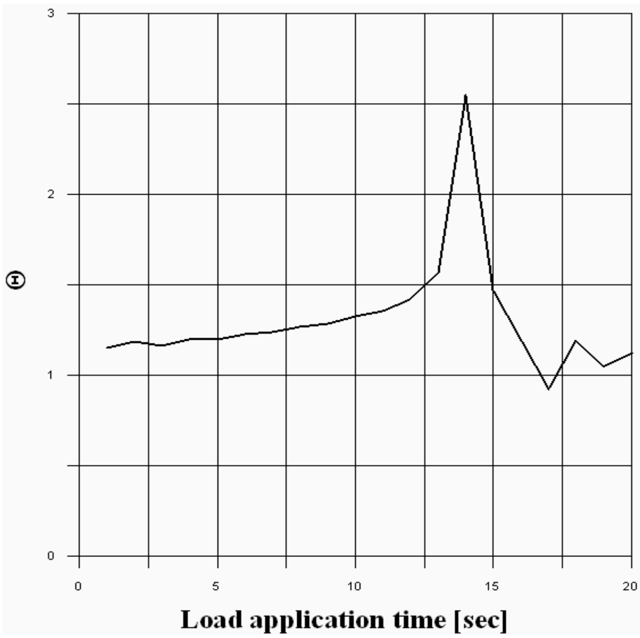

Fig. 16. Plot of the Θ norm (16)

References

[1] C. Calì, R. Esposito, M. Graziano, G. Russo, Numerical responses with finite displacements of axially compressed laminated panels, Italian-Polish Meeting on Analysis and Control of Complex Systems, Naples, November 1993.

[2] C. Calì, R. Esposito, M. Graziano, G. Russo, Geometrically non-linear analysis for some axially compressed laminated cylindrical panels, Applied Composite Materials, 1, 1994.

[3] C. Calì, F. Caputo Jr., G. Cricrì, R. Esposito, Analisi del comportamento in post-buckling di pannelli cilindrici laminati compressi assialmente, XXVI AIAS National Conference, 1997.

[4] C. Calì, R. Esposito, Some design problems and correlated numerical techniques, International Seminar on Principles and Methods of Engineering Design, Naples, October 1997.

[5] C. Calì, R. Esposito, Numerical Investigation on the Shear Buckling of Laminated Cylindrical Shells, 2nd AMME Conference, Gliwice, 1993.

[6] C. Calì, R. Esposito, Investigation on Buckling of Multi-layered Cylinders under Torsion, 14th AMME Conference, Zakopane, May 1995.

[7] C. Calì, R. Esposito, G. Godono, Improvement of Optimizing Procedures in Design of Multilayered Cylindrical Orthotropic Panels, 5th AMME Conference, Gliwice-Wisla, December 1996.

[8] C. Calì, F. Caputo jr, G. Cricrì, R. Esposito, Dynamic Analyses for Post-Buckling Behaviour, 7th AMME Conference, Gliwice-Zakopane, November 1998.

[9] E. Armentani, C. Calì, F. Caputo jr., R. Esposito, Influence of Curvature on Buckling Behaviuor of Aircraft Composite Panels, 8th AMME Conference, Gliwice-Rydzyna-Pawlowice-Rokosowo, October 1999.

[10] E. Armentani, F. Caputo jr., R. Esposito, Numerical simulation of a rolling process, 10th AMME Conference, Gliwice, December 2001.

[11] E. Armentani, A. De Martino, M. Pirozzi, A complete FE model for vehicle crashworthiness, 11th AMME Conference, Gliwice-Zakopane, December 2005.

[12] G. Forasassi, R. Lo Frano, Buckling of imperfect thin cylindrical shell under lateral pressure, Journal of Achivements in Materials and Manufacturing Engineering 18 (2006), 287-290.

[13] U. Lee, J. Cho, Dynamic response with arbitrary initial conditions using the FFT, Journal of Achivements in Materials and Manufacturing Engineering 18 (2006), 299-302.

[14] V. Mandic, M. Stefanovic, M. Zivkovic, N. Grujovic, B. Misic, FE analysis of tube forming process with experimental verification, Journal of Achivements in Materials and Manufacturing Engineering, 18 (2006), 303-306.

[15] J. B. Abrantes, A. Szabo-Ponce, G. F. Batalha , Experimental and numerical simulation of tube hydroforming (THF), Journal of Materials Processing Techonology 164-165 (2005) 1140-1147.

[16] M. Tahani, M.A. Torabizadeh, A. Fereidoon, Nonlinear analysis of functionally graded beams, Journal of Achivements in Materials and Manufacturing Engineering, 18 (2006), 315-318.

[17] Fuh-Kuo Chen, Shen-Fu Ko, Deformation analysis of springback in L-bending of sheet metal, Journal of Achivements in Materials and Manufacturing Engineering 18 (2006) 339-342.

[18] A. Gontarz, The new forging process of a wheel hub drop forging, Journal of Achivements in Materials and Manufacturing Engineering 18 (2006) 363-366.

[19] Z. Pater, Finite element analysis of cross wedge rolling, Journal of Materials Processing Technology 173 (2006), 201-208.

[20] T. Ohashi, H. Ito, K. Shinozaki, S.Ito, H. Watari, Analytical and experimental study on lateral extrusion of cross fitting with a lost core, Journal of Achivements in Materials and Manufacturing Engineering 18 (2006) 399-402.

[21] I. Pahole, M. Puc, B. Vaupotič, J. Balič, Comparison of technology of forming the sheet metal by numerical simulations, Journal of Achivements in Materials and Manufacturing Engineering 18 (2006) 403-406.

[22] E. Bayraktar, N. Isac, G. Arnold, Buckling limit diagrams (BLDs) of interstitial free steels (IFS): Comparison of experimental and finite element analysis, Journal of Materials Processing Technology 164–165 (2005) 1487–1494.

[23] M. S. Tehrani, H. M. Naeini, P. Hartley, H. Khademizadeh, Localized edge buckling in cold roll-forming of circular tube section, Journal of Materials Processing Technology 177 (2006) 617–620.

[24] F. Mao, J.H. Mo, S.H. Huang, Study on instability of the point bolster sheet metal dieless forming, Journal of Materials Processing Technology 176 (2006) 13–18.

[25] C.S. Namoco Jr., T. Iizuka, R.C. Sagrado, N. Takakura, K. Yamaguchi, Experimental and numerical investigation of restoration behavior of sheet metals subjected to bulging deformation, Journal of Materials Processing Technology 177 (2006) 368–372.

[26] Yuung-Ming Huang, Finite element analysis of tube inward curling process by conical dies, Journal of Materials Processing Technology 170 (2005) 616–623.

[27] M.L. Alves, B.P.P. Almeida, P.A.R. Rosa, P.A.F. Martins, End forming of thin-walled tubes, Journal of Materials Processing Technology 177 (2006) 183–187.

[28] S.C. Heo, J. Kim, B.S. Kang, Investigation on determination of loading path to enhance formability in tube hydroforming process using APDL, Journal of Materials Processing Technology 177 (2006) 653–657.

[29] M.P. Lightfoot, N.A. McPherson, K. Woods, G.J. Bruce, Artificial neural networks as an aid to steel plate distortion reduction, Journal of Materials Processing Technology 172 (2006) 238–242.

[30] G.A. Wempner, Discrete approximation related to non-linear theories of solids, International Journal of Solids & Structures 7 (1971) 1581-1599.

[31] E. Riks, The application of Newton's method to the problems of elastic stability, Journal of Applied Mechanics 39 (1972) 1060-1066.

[32] E. Riks, An incremental approach to the solution of snapping and buckling programs, International Journal of Solids & Structures 15 (1979) 529-551.

[33] G. Cricrì, Metodi di analisi via FEM del comportamento critico e post – critico di strutture elastiche – PhD thesis, march 1998.

[34] C. Calì, F. Caputo Jr., G. Cricrì, R. Esposito. Dynamic analyses for post buckling behaviour, 7th AMME Conference, Zakopane, 1998.

[35] A. Apicella, E. Armentani, C. Calì, F. Caputo, R. Esposito, Buckling and Post- Buckling Analyses of a GLARE Thick Flat Side Panel, ETC/OMAE 2000 Joint Conference, New Orleans, LA, February 2000.

[36] M.A. Crisfield, A fast Incremental iterative Solution Procedure that handles "Snap-Through" - Computer & Structures 13 (1981) 55-62.

[37] M.A. Crisfield, Non-Linear Finite Element Analysis of Solid and Structures - Vol. I, John Wiley & Sons, Chichester, 1991.
[38] M.A. Crisfield, Non-linear finite element analysis of solids and structures Vol. 1: Essentials, John Wiley & Sons, Chichester, 1997.
[39] M.A. Crisfield, Non-linear finite element analysis of solids and structures Vol. 2: Advanced Topics, John Wiley & Sons, Chichester, 1997.
[40] H. Hellweg, M.A. Crisfield, A new Arc Length method for handling sharp snap-back. Computer & Structures, 66 (1998) 705-709.
[41] B.W.R. Forde and S.F. Stiemer, Improved Arc Length orthogonality methods for non-linear finite element analysis, Computer & Structures, Vol. 27, N° 5 (1987) 625-630.
[42] K.S. Surana, Geometrically non-linear formulation for the curved shell element, International Journal of Numerical Methods for Engineering, 19 (1983).
[43] O.C. Zienkiewicz and R.L. Taylor, The Finite Element Method, Vol. 2, McGraw-Hill Book Company, London, 1991.
[44] Ansys 5.7 On Line User’s Manual, ANSYS Inc., 2000.